The Effect of Chloride Ions Concentration on the Electrochemical Behavior of AISI 410 Stainless Steels in Simulated Concrete Pore Solution

A. Fattah-alhosseini[1]* , M. Hojati Fahim[2], E. Nikomanzari[3]

Department of Materials Engineering, Bu-Ali Sina University, Hamedan 65178-38695, Iran

Abstract

The effect of chloride ions concentration on the electrochemical behavior of AISI 410 stainless steel in the simulated concrete pore (0.1 M NaOH + 0.1 M KOH) solution was investigated by various electrochemical methods such as Potentiodynamic polarization, Mott–Schottky analysis and electrochemical impedance spectroscopy (EIS). Potentiodynamic polarization curves revealed that increasing chloride ions concentration led to decreasing the corrosion and pitting potentials of AISI 410 stainless steel. Mott–Schottky analysis demonstrated that passive films formed on AISI 410 stainless steel in the simulated concrete pore solution with and without NaCl addition showed some n-type semiconducting behavior in nature. Moreover, Mott–Schottky results showed that the donor density was increased by increasing chloride ions concentration. EIS revealed that in the absence of chloride ions, the surface films formed on AISI 410 stainless steel in the simulated concrete pore showed higher passive film and charge transfer resistance. However, in the presence of chloride ions, an inversion of this trend was observed.

Keywords: AISI 410 stainless steel; Chloride ion; Concrete; Polarization.

1. Introduction

Martensitic stainless steels (especially AISI 410) are mainly used for applications where high strength is required. However, due to their low chromium content, these stainless steels are relatively sensitive to corrosion [1-5]. Generally, the corrosion resistance of stainless steels is due to the presence of passive films formed on the surface. The nature and content of alloying elements and specific experimental conditions (neutral, acidic or alkaline) affect the chemical composition and the structure of the passive films [6-8]

The passive films are made of oxides or hydroxides identified as semiconductors. Semiconducting properties are then observed on the passive films. To come to a better understanding of passive films formed on stainless steels, many studies have been performed on semiconducting properties through Mott–Schottky analysis [9-14]. In recent years, many studies on semiconducting properties of passive films formed on stainless steels have led to a better understanding of the corrosion behavior of these alloys [15-18].

Generally, the chemical composition of passive films varies with alloy composition and pH of the solution, while it is expected to affect semiconducting properties of the film [19, 20]. In alkaline solutions, the main effect of increasing pH on film formation is thickening the passive film, because iron oxides are more stable in these solutions [21]. Conversely, in acidic solutions, chromium-rich oxide film is formed due to the slower dissolution of chromium oxide when compared to iron oxide [22].

Although many studies have been published on the passivity of stainless steels in alkaline solutions, there is little information regarding the effect of chloride concentration on the semiconducting behavior of the passive film formed on these alloys in these solutions. At first, the present work was designed to better understand the electrochemical behavior of AISI 410 martensitic stainless steel in the simulated concrete pore (0.1 M NaOH + 0.1 M KOH) solution. Moreover, the Mott–Schottky analysis of this stainless steel in the simulated concrete pore with and without NaCl addition at open circuit potential (OCP) conditions was performed to determine the semiconducting behavior. In addition, estimation of the dopant levels in the passive film and the assessment of the dopant levels in the film as a function of chloride ions concentration were done in this study.

2. Experimental Procedures

The specimens were fabricated from a thick plate of AISI 410 stainless steel with the chemical composition (%, wt.): Cr 19.1, Ni 9.35, Mn 1.66, Si 0.45, C 0.08, P 0.03, S 0.003, and balance Fe. All samples were ground to 2000 grit and cleaned by deionized water prior to tests. The solutions used in this study

* *Corresponding author*
Tel: +98 813 8252505   Fax: +98 813 8257400
E-mail: a.fattah@basu.ac.ir
Address: Department of Materials Engineering, Bu-Ali Sina University, Hamedan 65178-38695, Iran
1. Assistant Professor
2. BSc
3. BSc

were 0.1 M NaOH + 0.1 M KOH (the simulated concrete pore) with and without NaCl addition (1.0%, 2.0%, 3.0% and 4.0% wt NaCl). The electrochemical measurements were performed in the following sequence:

(a) Potentiodynamic polarization curves were measured potentiodynamically at a scan rate of 1 mV s^{-1} by starting from -0.25 V (vs. E_{corr}).

(b) Mott-Schottky analysis was carried out on the passive films at a frequency of 1 kHz using a 10 mV ac signal and a step potential of 25 mV, in the cathodic direction.

(c) EIS test was conducted at OCP DC potential, AC potential with the amplitude of 10 mV and normally, a frequency range of 100 kHz to 10 mHz.

Prior to all electrochemical measurements, working electrodes were immersed at OCP in solutions to form a steady-state passive film. All electrochemical measurements were performed in a conventional three-electrode flat cell. The counter electrode was a Pt plate, and all potentials were measured against Ag/AgCl in saturated KCl. All electrochemical measurements were obtained using Autolab potentiostat/ galvanostat controlled by a personal computer. For EIS data modeling and curve-fitting method, the NOVA impedance software was used.

3. Results and discussion
3.1. Open circuit potential (OCP) measurements

In Fig. 1, changes in OCP of AISI 410 stainless steel in the simulated concrete pore solution with and without NaCl addition are shown. At the start of immersion, the potential was immediately reduced, showing the dissolution of oxide layer for all solutions. However, as time passed, the open circuit potential was directed towards the positive amount. Fig. 1 also indicates that within 1500 seconds, a stable condition was achieved and electrochemical tests could be conducted.
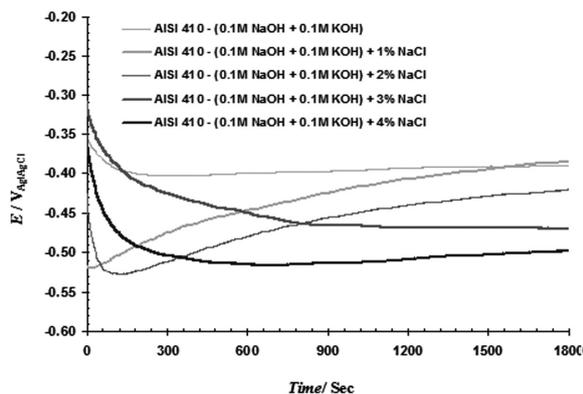

Fig.1. OCP plots of AISI 410 stainless steel in 0.1 M NaOH + 0.1 M KOH solution with and without NaCl addition. Fig.1. OCP plots of AISI 410 stainless steel in 0.1 M NaOH + 0.1 M KOH solution with and without NaCl addition.

3.2. Potentiodynamic polarization measurements

Fig. 2 shows the potentiodynamic polarization curves for AISI 410 stainless steel in the simulated concrete pore solution with and without NaCl addition. It could be observed that the electrodes exhibited the same curve shapes, where the current was changed smoothly and linearly around the rest potential, thereby manifesting cathodic and anodic Tafel behavior. Also, no active-passive transition peak was observed in the anodic curve. As illustrated, the passive current density was enhanced with the increase in the concentration of chloride ions.
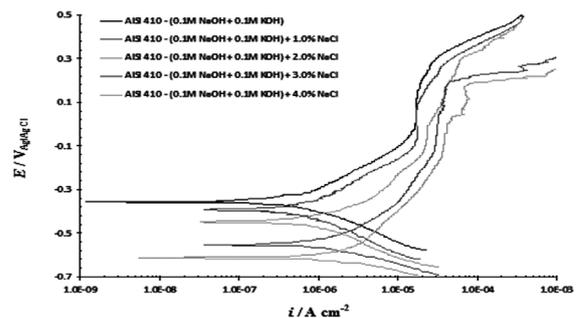

Fig.2. The effect of chloride ions concentration on the potentiodynamic polarization curve of AISI 410 stainless steel in 0.1 M NaOH + 0.1 M KOH solution.

The corrosion current density (i_{corr}) was calculated by Tafel extrapolation of the linear part for the cathodic branch back to the corrosion potential [23]. The variations of the corrosion current density of AISI 410 stainless steel in the simulated concrete pore solution with and without NaCl addition are illustrated in Fig. 3.
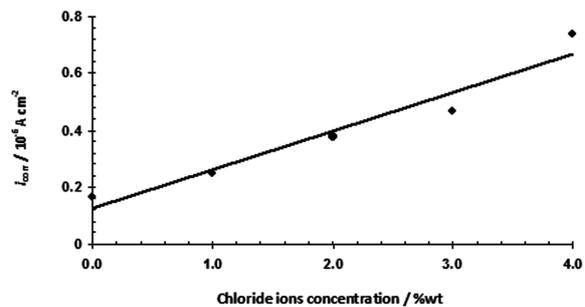

Fig.3. Variations of the corrosion current density of AISI 410 stainless steel in 0.1 M NaOH + 0.1 M KOH solution with and without NaCl addition.

It could be observed that the corrosion current density of AISI 410 stainless steel was increased linearity with the increase in the concentration of chloride ions. Also, variations in the corrosion and pitting potentials of this stainless steel in the simulated concrete pore solution with NaCl addition are shown in Fig. 4. As can be seen, the corrosion and pitting potentials of this stainless steel were decreased with the increase in the concentration of chloride ions. Also as can be

seen in Fig.4 (a), corrosion potentials determined according to potentiodynamic polarization curves were different from the OCP plots. These differences were correlated to the partial reduction of metal ions in the passive film after applying the cathodic polarization step during potentiodynamic polarization measurements. Moreover, the chemical composition and structure of the passive films were changed by increasing the potential. Thus, the corrosion potentials were shifted to more negative regions during the potentiodynamic polarization measurements as compared to the rest potentials obtained from OCP plots [24].

Fig.5. Mott-Schottky plots of passive film formed on AISI 410 stainless steel in 0.1 M NaOH + 0.1 M KOH solution with and without NaCl addition.

It has been reported the first and second slopes correlated with Fe^{2+} are located in the tetrahedral and octahedral sites of a spinel type structure, respectively [9]. Generally, it has been shown that Mott-Schottky plots obtained for bulk metal oxides like Fe_2O_3 show no breakdown of linearity, and the n-type semiconducting behavior is correlated with the presence of Fe^{2+} ions that act as donor levels [25]. However, for passive films formed on pure iron or stainless steels, the origin of the two slopes has been observed in the passive region [26, 27].

As can be seen in Fig. 5, capacitances were clearly increased with the increase in the concentration of chloride ions. According to Eq. (1), donor density was determined from the positive slope [9-13]:

$$\frac{1}{C_{SC}^2} = \frac{2}{\varepsilon\varepsilon_0 e N_D}\left(E - E_{FB} - \frac{k_B T}{q} \right) \tag{1}$$

where e is the electron charge, N_D represents the donor density for n–type semiconductors (cm^{-3}), ε stands for the dielectric constant of the passive film (usually taken as 15.6 for stainless steels), ε_0 denotes the vacuum permittivity, and k, T, and E_{FB} are the Boltzmann constant, absolute temperature, and flat band potential, respectively [9-13].

Fig. 6 displays the calculated donor density of passive films formed on AISI 410 stainless steel in the simulated concrete pore solution with and without NaCl addition. These values were correlated with densities close to the stainless steel/passive film interface, where the concentrations of oxygen vacancies and metal interstitials were predicted to be the highest. It was observed that N_D was increased with increasing chloride ions concentration. Indeed, the addition of chloride ions to the simulated concrete pore solution increased the incorporation of chloride ions into the passive film, by which the additional charge carriers were generated [28].
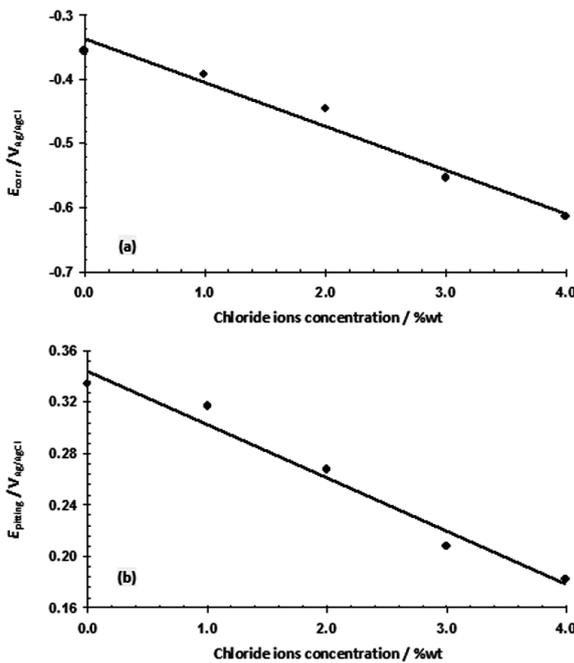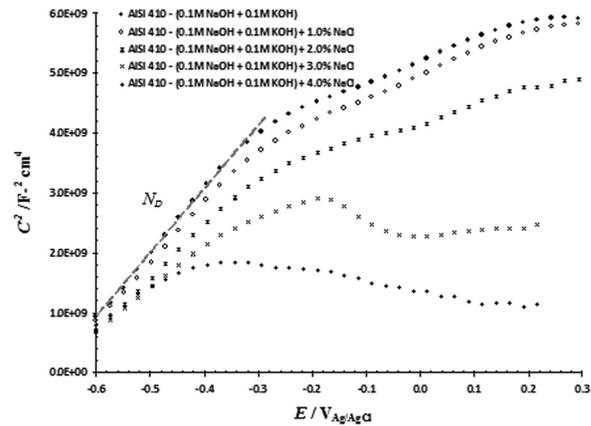

Fig.4. The effect of chloride ions concentration on the (a) corrosion and (b) pitting potential of AISI 410 stainless steel in 0.1 M NaOH + 0.1 M KOH solution.

3.3. Mott–Schottky analysis

Generally, more detailed evidence regarding the nature of passive films was obtained using Mott–Schottky analysis. Fig. 5 represents the Mott-Schottky plots for passive films formed on AISI 410 stainless steel in the simulated concrete pore solution with and without NaCl addition.

All plots showed two regions with the positive slope (except in the simulated concrete pore solution with 3.0 and 4.0 wt% NaCl), in which a linear relationship between C^{-2} and E could be observed. These plots demonstrated that passive films formed on AISI 410 stainless steel showed some n-type semiconducting behavior, where the oxygen vacancies and interstitials were preponderated over the cation vacancies.
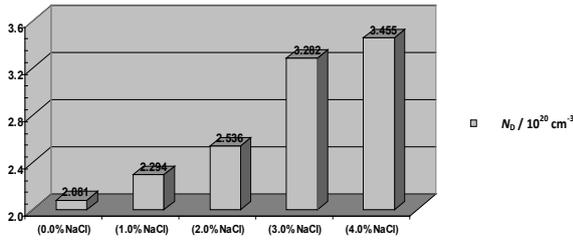
Fig.6. Variations of the donor densities of passive films formed on AISI 410 stainless steel in 0.1 M NaOH + 0.1 M KOH solution with and without NaCl addition.

Point defect Model (PDM) postulates that point defects present in the passive film are, in general, cation vacancies (V_M^χ), oxygen vacancies ($V_O^{\cdot\cdot}$), and cation interstitials ($M_i^{\chi+}$). In this study, the dominant point defects were oxygen vacancies and cation interstitials acting as electron donors at the passive film/solution interface [15, 16]. Therefore, in the concentrated solutions, the chloride ions (Cl^-) could be absorbed into the oxygen vacancies [28, 29]:

$$V_O^{\cdot\cdot} + Cl^- \cdot nH_2O \rightarrow Cl_O^{\cdot} + nH_2O \qquad (1)$$
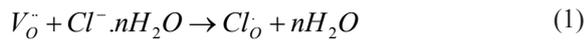
where $Cl_O^{\cdot}$ is a chloride ion occupying an oxygen lattice site. This reaction allowed the generation of cation vacancy/oxygen vacancy pairs at the passive film/solution interface through the Schottky-pair reaction:

$$Null \rightarrow V_M^\chi + \left(\frac{\chi}{2}\right)V_O^{\cdot\cdot} \qquad (2)$$

It became clear that chloride ion absorption led to the generation of cation vacancies at the passive film/solution interface, thereby resulting in the flux of cation vacancies across the passive film to the passive film/metal interface. The cation vacancies were annihilated at the metal/passive film interface by emitting cations from the metal into the passive film as follows:

$$m + V_M^{\chi'} \rightarrow M_M + V_m + \chi e' \qquad (3)$$
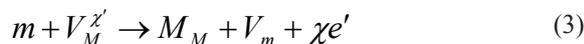
where m is a metal atom, M_M is a metal cation in a cation site and V_m is a vacancy in the metal phase. It can be understood that if this annihilation reaction can not consume the cation vacancies arrived, the excess vacancies will be condensed at the metal/passive film interface. As the vacancy condensate grows to a critical size, it will successively result in the formation of voids at the metal/film interface. Generally, the cation vacancies and cation interstitials experience anion-catalyzed reaction processes which may cause not only the formation of interfacial void and the ensuing rupture of local film, but also the local thinning of the passive film. It should be noted that both the voiding process at the metal/passive film interface and the

thinning process at the passive film may take place simultaneously, and they are responsible for the local depassivation and the initiation of the pitting corrosion on the less resistive sites of the passive film [28, 29].

The local depassivated sites may grow as stable pits or they may be repassivated as metastable pits, depending on the key environmental parameters (especially chloride ions concentration) [28, 29]. Therefore, with increasing the chloride ions concentration, N_D was increased in the passive film (Fig. 6), whereas the number of absorbed anions could become larger through promoting the reaction Eq. (1). It is believed that the reaction rates of the anion-catalyzed reactions (Eqs. (1) to (3)) are accelerated by the increase of N_D in the passive film. Subsequently, the voiding and/or thinning processes may be enhanced to deteriorate the stability of the passive film. Therefore, the pitting susceptibility of AISI 410 stainless steel in the simulated concrete pore was increased with the chloride ions concentration, as characterized by the $E_{pitting}$ values in Fig. 4(b).

3.4. EIS measurements

Fig. 7 presents the Nyquist and Bode plots of AISI 410 stainless steel in the simulated concrete pore solution with and without NaCl addition. As shown in Nyquist and Bode plots (Figs. 7a and 7b), the overall impedance (especially in the low frequency domain) was decreased with the increase in the concentration of chloride ions. As shown in Bode phase plots (Fig. 7c), the phase angle maxima was lower than 90°. Such a behavior can be explained as a deviation from the ideal capacitor behavior. Also, these plots do not show one time constant. Similar Nyquist and Bode plots with two times constant have been observed for other stainless steels in the simulated concrete pore [30-33]. Therefore, the equivalent circuit shown in Fig. 8 was used to simulate the measured impedance data on AISI 410 stainless steel in the simulated concrete pore solution with and without NaCl addition.

It should be added that this equivalent circuit presents two time constants. The first time constant in high frequency (R_{pf} and Q_{pf}) reveals the information of the passive film. Moreover, the second time constant in low frequency (R_{ct} and Q_{dl}) is correlated with the film defects in the absence of chloride ions, and active pits and film defects in the presence of chloride ions. Also, R_s in high frequency is the solution resistance. Fig. 9 shows the evolution of the passive film resistance (R_{pf}) and charge transfer resistance (R_{ct}) as a function of chloride ions concentration. As shown, the passive film resistance (R_{pf}) and charge transfer resistance (R_{ct}) were decreased with the increase in the concentration of chloride ions. Indeed, in the absence of chloride ions, the surface films formed on AISI 410 stainless steel in the simulated

concrete pore showed higher passive film and charge transfer resistance. However, in the presence of chloride ions, an inversion of this trend was observed.
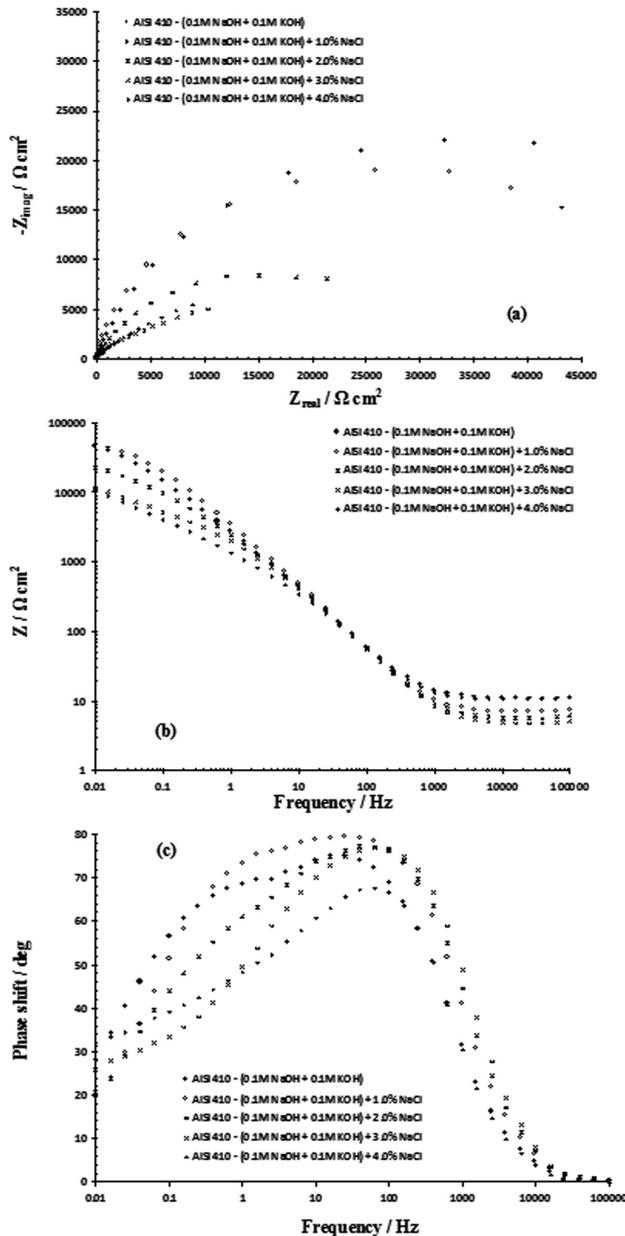

Fig.7. Nyquist and Bode plots of AISI 410 stainless steel in 0.1 M NaOH + 0.1 M KOH solution with and without NaCl addition.
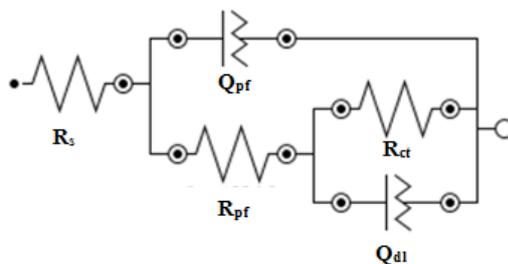

Fig.8. Best equivalent circuit used to model the experimental EIS data of AISI 410 stainless steel in 0.1 M NaOH + 0.1 M KOH solution with and without NaCl addition.
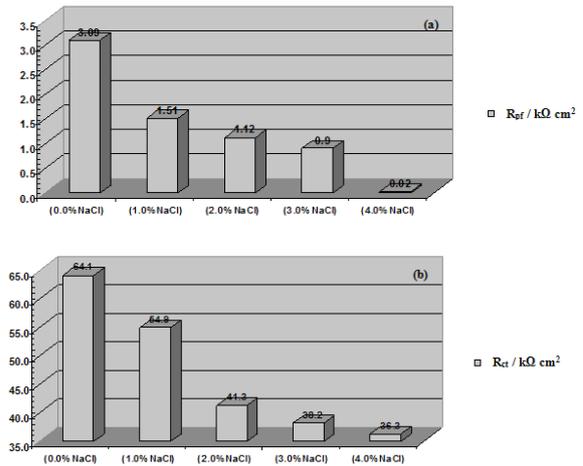

Fig.9. Variations of the (a) passive film resistance and (b) charge transfer resistance as a function of chloride ions concentration.

4. Conclusions

Electrochemical behavior of AISI 410 stainless steel in simulated concrete pore solution with and without NaCl addition was studied in the present work. Conclusions drawn from the study are as follows:

1. Potentiodynamic polarization curves indicated that increasing chloride ions concentration led to increasing the corrosion current density of AISI 410 stainless steel in the simulated concrete pore solution.

2. The decrease of corrosion and pitting potentials of AISI 410 stainless steel in the simulated concrete pore solution was observed when the concentration of chloride ions was increased.

3. Mott–Schottky analysis demonstrated that the passive films formed on AISI 410 stainless steel showed the n-type semiconducting behavior, where the oxygen vacancies and interstitials were preponderated over the cation vacancies.

4. Also, the Mott–Schottky results showed that donor densities obtained from the Mott–Schottky plots were in the range of 10^{20} cm^{-3} and they were increased with increasing chloride ions concentration.

5. EIS revealed that in the absence of chloride ions, the surface films formed on AISI 410 stainless steel in the simulated concrete pore showed higher passive film and charge transfer resistance. However, in the presence of chloride ions, an inversion of this trend was observed.

References

[1] C.A. Gervasi, C.M. Méndez, P.D. Bilmes, C.L. Llorente: Mater. Chem. Phy., 126 (2011), 178.

[2] C.A. Gervasi, P.D. Bilmes, C.L. Llorente: Corrosion Research Trends, Nova Science Publishers, NY, (2007).

[3] P.D. Bilmes, C.L. Llorente, C.M. Méndez, C.A. Gervasi: Corros. Sci., 51 (2009), 876.

[4] D. Thibault, P. Bocher, M. Thomas: J. Mater. Process. Tech., 209 (2009), 2195.

[5] X.P. Ma, L.J. Wang, C.M. Liu, S.V. Subramanian: Mater. Sci. Eng. A, 539 (2012), 271.

[6] T. Ohtsuka, H. Yamada: Corros. Sci., 40 (1998), 1131.

[7] J.S. Kim, E.A. Cho, H.S. Kwan: Corros. Sci., 43 (2001), 1403.

[8] N. Le Bozec, C. Compère, M. L'Her, A. Laouenan, D. Costa, P. Marcus: Corros. Sci., 43 (2001), 765.

[9] N.E. Hakiki, M. Da Cunha Belo, A.M.P. Simões, M.G.S. Ferreira: J. Electrochem. Soc., 145 (1998), 3821.

[10] M. Da Cunha Belo, N.E. Hakiki, M.G.S. Ferreira: Electrochim. Acta, 44 (1999), 2473.

[11] M.F. Montemor, A.M.P. Simões, M.G.S. Ferreira, M. Da Cunha Belo: Corros. Sci., 41 (1999), 17.

[12] J. Amri, T. Souier, B. Malki, B. Baroux: Corros. Sci., 50 (2008), 431.

[13] S. Ningshen, U. K. Mudali, V.K. Mittal, H.S. Khatak: Corros. Sci., 49 (2007), 481.

[14] K. Sugimoto, Y. Sawada: Corros. Sci., 17 (1997), 425.

[15] A. Fattah-alhosseini, F. Soltani, F. Shirsalimi, B. Ezadi, N. Attarzadeh: Corros. Sci., 53 (2011), 3186.

[16] A. Fattah-alhosseini, M.A. Golozar, A. Saatchi, K. Raeissi: Corros. Sci., 52 (2010), 205.

[17] M. Yazıcı, O. Çomaklı, T. Yetim, A.F. Yetim, A. Çelik: Surf. Coat. Techn., 261 (2015), 181.

[18] N.E. Hakik: Corros. Sci., 53 (2011), 2688.

[19] C. Sunseri, S. Piazza, F. Di Quarto: J. Electrochem. Soc. 137 (1990), 2411.

[20] M.J. Carmezim, A.M. Simões, M.O. Figueiredo, M. Da Cunha Belo: Corros. Sci., 44 (2002), 451.

[21] S. Haupt, H.-H. Strehblow: Corros. Sci., 37 (1995), 43.

[22] M.V. Cardoso, S.T. Amaral, E.M.A. Martini: Corros. Sci., 50 (2008), 2429.

[23] G.T. Burstein: Corros. Sci., 47 (2005), 2858.

[24] S. Tait: An introduction to electrochemical corrosion testing for practicing engineers and scientists. USA: PairODocs Publications; (1994).

[25] P. Schmuki, M. Büchler, S. Virtanen, H. Böhni, R. Müller, L.J. Gauckler: J. Electrochem. Soc., 142 (1995), 3336.

[26] E. Sikora, D.D. Macdonald: J. Electrochem. Soc., 147 (2000), 4087.

[27] F. Gaben, B. Vuillemin, R. Oltra: J. Electrochem. Soc., 151 (2004), B595.

[28] Z. Jiang, X. Dai, T. Norby, H. Middleton: Corros. Sci., 53 (2011), 815.

[29] D.D. Macdonald: Pure Appl. Chem., 71 (1999), 951.

[30] L. Freire, M.J. Carmezim, M.G.S. Ferreira, M.F. Montemor: Electrochim. Acta, 56 (2011), 5280.

[31] L. Freire, M.J. Carmezim, M.G.S. Ferreira, M.F. Montemor: Electrochim. Acta, 55 (2010), 6174.

[32] H. Luo, C.F. Dong, X.G. Li, K. Xiao: Electrochim. Acta, 64 (2012), 211.

[33] R. Liu, L. Jiang, J. Xu, C. Xiong, Z. Song: Constr. Build. Mater., 56 (2014), 16.